# A Tough Reversible Biomimetic Transparent Adhesive Tape with Pressure-sensitive and Wet-cleaning Properties

*Ming Li*[†,*,a], *Weijun Li*[†,*,b], *Qingwen Guan*[c], *Jing Lv*[d], *Eduardo Saiz*[a]

[a] Centre of Advanced Structural Ceramics, Department of Materials, Imperial College London, London, SW7 2AZ, UK. Email: m.li19@imperial.ac.uk
[b] State Key Laboratory of Physical Chemistry of Solid Surfaces, College of Chemistry and Chemical Engineering, Xiamen University, Xiamen 361005, China. Email: lwjdesky@163.com
[c] School of Chemistry, University of Glasgow, Glasgow, G12 8QQ, UK
[d] College of New Energy and Materials Science, China University of Petroleum (Beijing), Beijing 102249, China.
† *These two authors contribute equally to this work.*

**Abstract:** Dry adhesives that combine strong adhesion, high transparency, and reusability are needed to support new developments in emerging fields such as medical electrodes and or electronic optical devices. However, to achieve all these features in a single material remains challenging. Herein, we proposed a pressure-responsive PU adhesive inspired by the octopus sucker. This adhesive not only showcases excellent reversible adhesion to both solid materials and biological tissues, but also exhibits stable and high transparency (>90%). As the adhesion strength could be adjusted by the joining force/pressure. The high static adhesion (~120 kPa) and 180° peeling force (~500 N/m) are higher than for most existing artificial adhesives. Moreover, the adhesion strength is effectively maintained even after 100 bonding-debonding cycles. Since the adhesive tape relies on the combination of negative pressure and intermolecular forces, it overcomes the problems caused by glue residues as those left by traditional glue tapes after removal. In addition, the PU adhesive also exhibits superior wet-cleaning performance, the contaminated tape can recover 90-95% of the adhesion strength by cleaning water. The results open new opportunities for the design and preparation of tapes with high reversible adhesion and long fatigue life.

**Keywords:** reversible, adhesive tape, bio-inspired, wet-cleaning, pressure-sensitive

## Introduction:

Natural evolution has created numerous adhesive structures exhibiting unique capabilities and reversible bonding. Typical examples include the feet of species as diverse as geckos, spiders or bettles,[1,5,7] or the suckers of octopus [2, 3] between others. Among them, gecko soles have received widespread attention due to their strong and long-lasting adhesion, easy detachment, and dry self-cleaning capabilities.[1, 6, 7] Relying on these seemingly contradictory properties, geckos can climb on various surfaces.[8] The strong adhesion of their feet derives from the Van der Waals forces arising from thousands of tiny bristles.[1, 9] Mimicking this mechanism, a large number of strong dry adhesives have been developed using microarray structures built on the surface of soft viscoelastic polymers.[3, 8, 10-13] These new biomimetic dry adhesives can bond to complex organic or inorganic surfaces, and have broad application prospects from biomedical adhesives, to climbing robots, electronic equipment bonding, or high-performance brakes. [14-18]

Traditional strategies for building microarray structures include electron beam lithography,[19] nanoimprinting,[20] nanomolding of polymer pillars,[21] soft lithography of biological structures,[22] chemical vapor deposition of carbon nanotubes,[23] and 3D direct Laser writing.[24] Ultimately, it is difficult to increase significantly the actual contact area between the substrate and the highly flexible artificial polymers using arrays with single-layer structures, what limits adhesion.[25] An alternative is to prepare multi-layer hierarchical structures that will increase contact area exponentially generating strong bonding on rough substrates.[1, 9, 26, 27] However, due to the mutual interaction between the different features at multiple length scales, these hierarchical microstructures are prone to collapse or buckle in practical applications, weakening adhesion .[10, 28] As a result, although the adhesion of some artificial dry adhesives far exceeds that of gecko feet, their durability and reusability are limited. For example, the adhesion of the biomimetic surfaces built using carbon nanotubes (CNTs) can reach 10

times than that of gecko feet.[23] However, after several bonding -debonding cycles the carbon nanotubes tend to fracture and plastic deformation, which degrades adhesion.[23] Moreover, dust contamination also has a detrimental effect on bonding.[29] The aim of this work is to develop a new strategy for the design and fabrication of dry, strong adhesives that can be easily cleaned and reused.

In this work, we describe a transparent, non-toxic and recyclable biomimetic polyurethane (PU) adhesive. Its strong adhesion mainly depends on the negative pressure effect (similar to the octopus sucker) and the various intermolecular forces between the adhesive and the solid surfaces. This adhesion mechanism effectively overcomes the problems of caused by fracture during removal observed in gecko-inspired dry adhesives. The PU adhesive maintains its strong adhesion even after one hundred bonding-debonding cycles at working temperatures ranging from -3 °C to 72 °C. This adhesive can adhere to various organic and inorganic solid surfaces, including ceramics, glass, polymers, wood, and metals, and also exhibits outstanding bonding to biological tissues such as fascia, fat, epidermis and muscle. In addition, the pressure applied during joining can be used to manipulate adhesion. More importantly, it exhibits a superior wet-cleaning capability, a contaminated PU adhesive recovers 90%-95% of its adhesion strength after rinsing with water. These unique properties create opportunities for the use of the PU adhesive in a wide variety of fields, including wound patches, medical electrodes, tissue adhesives and portable devices.

## Results and Discussion

In this work we describe the design and fabrication of a biomimetic, strong and pressure-responsive polyurethane adhesive (Figure S1, Video S1). The synthesis and internal structure of the adhesive tape are described in Figure 1a. The covalent bond (-CONH-, Figure S2), formed through the nucleophilic

addition of isocyanate groups and polyether polyols during the crosslinking reaction, can effectively lock the adhesive's inner chains and give the PU adhesive some tensile strength and mechanical stability (Video S2). However, the weaker bonds such as the π-π conjugation, hydrogen bonding and chain entanglement in the network break during stretching and re-form during retraction (Figure S3). The process of bond breaking and re-forming at different locations lead to permanent, plastic deformation when the external force is removed (Figure S4, Video S2).

If pressure is applied to the adhesive during bonding, it will deform to fit more closely on the solid surface. This deformation will remain after the removal of the force, thereby increasing the actual contact area between adhesive and substrate (Figure S5). Moreover, a large number of micro/nano pores filled with air, are distributed on the surface of the PU adhesive (Figure S6). When the joining force is large enough, the air in these pores would be removed generating a negative pressure that increases the adhesion strength. On the other hand, the -NH, C═O and unsaturated benzene ring structures in the PU adhesive could also increase bonding between the adhesive and solid surfaces (Figure S3 and Figure 1c).[30, 31]

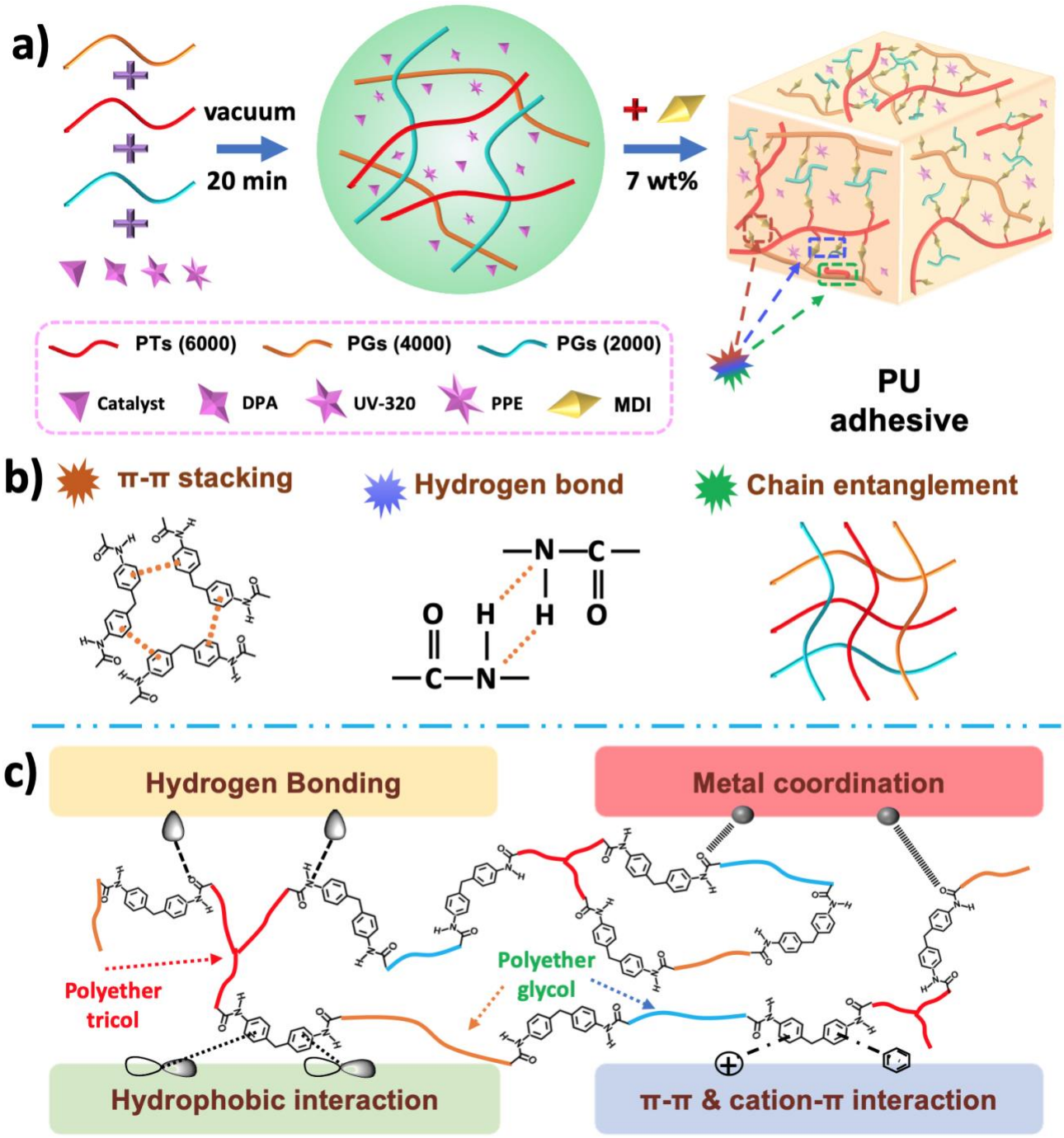


**Figure 1.** a) Schematic of the preparation of PU adhesive. b) Internal interactions in the material. c) Possible adhesion mechanisms between PU adhesives and solid surfaces.

**Adhesion performance**

To accurately evaluate the performance of the PU adhesive on a glass substrate, we tested its static adhesion strength and 180° peeling force (Figure S7). The adhesion performance is closely related to the joining pressure (Figure 2a). It increases with increasing force and saturates at about 400 kPa.

Following these results we chose a joining pressure of 500 kPa to compare adhesion measurements. We also investigated the adhesion performance of typical commercial adhesive tapes, including 3M VHB tape, PVC tape, Kapton tape, traditional double-sided tape and 3M magic tape (Figure S8). As shown in Figures 2b and 2c, the PU adhesive exhibits stronger static adhesion strength (~120 kPa) and 180° peeling force (~500 N/m) than commercially available adhesive tapes. What's more, its adhesion is far stronger than that of most reported artificial dry adhesives.[32]

The PU adhesive not only exhibits excellent static/peeling adhesion in a wide range of organic and inorganic solid surfaces (Figure S9); it also lefts no residue when the tape is peeled off (Figure S10). In addition, the tape also shows outstanding adhesion to biological tissues such as epidermis, fascia, fat and muscle (Figure S11-12). Figure 2d summarizes the static adhesion strength and 180° peeling force of the PU adhesive to several representative surfaces. Bonding is strongest on the aluminum alloy due to the effect of metal complexation and hydrogen bonding.[30] The physical interactions between the PU adhesive tape and glass, ceramic or rubber are dominantly hydrogen bonding or hydrophobic interactions, so the adhesion strength is weaker than that of aluminum alloy.[30] Porcine skin, secretes grease and impairs the negative pressure effect of the PU adhesive, therefore adhesion is significantly lower than on other solid surfaces.

The PU adhesive is also highly reusable. Taking the glass surface as an example, the performance of the adhesive remains stable even after 100 bonding-debonding cycles (Figure 2e). In addition, the adhesion strength after the first removal does not depend on the time that the PU remained bonded to the surface in the first cycle. (Figure 2f). The stable working temperature range of the PU adhesive is −3 °C to 72 °C (Figure 2g). If the temperature is too low, moisture in the air will condense on the

adhesive's surface, forming a layer of water that decreases the strength. If it is too high, the PU adhesive melts and cannot be reused, although the adhesion is enhanced.

Another interesting feature of the PU adhesive is its dynamic adhesion capability: the adhesive tape could stretch or contract with the surface to which is attached. When the limb undergoes repetitive contraction or stretching, the PU adhesive would firmly adhere to the skin instead of slipping or falling off (Figure S13 and Video S3). This is mainly due to its ability to stretch consequence of the relatively weak, reversible bonds. It can be seen from Figure 2h that the adhesive tape would elongate when it suffers external force. Therefore, as long as the transverse shear force generated during the limb's movement is lower than the static adhesion strength of PU adhesive (120 kPa), the adhesive tape could move with the skin without detachment. Since the tensile stress >> static adhesion strength, the tape would not break during the movement. Moreover, after 24 hours of adhesion, the skin didn't show any allergic symptoms (Figure S14). Further cytotoxicity experiments revealed that the PU adhesive is non-toxic (Figure S15 and Tables S1 and S2), making it potentially useful in applications such as medical electrodes, joint connections of wearable devices. To investigate the viscoelastic characteristics of the PU adhesive, we performed oscillatory rheology testing (Figure 2i). As expected, the adhesive displayed plastic deformation behavior when the strain is higher than 5%, with the storage modulus ($G'$) < loss modulus ($G''$).

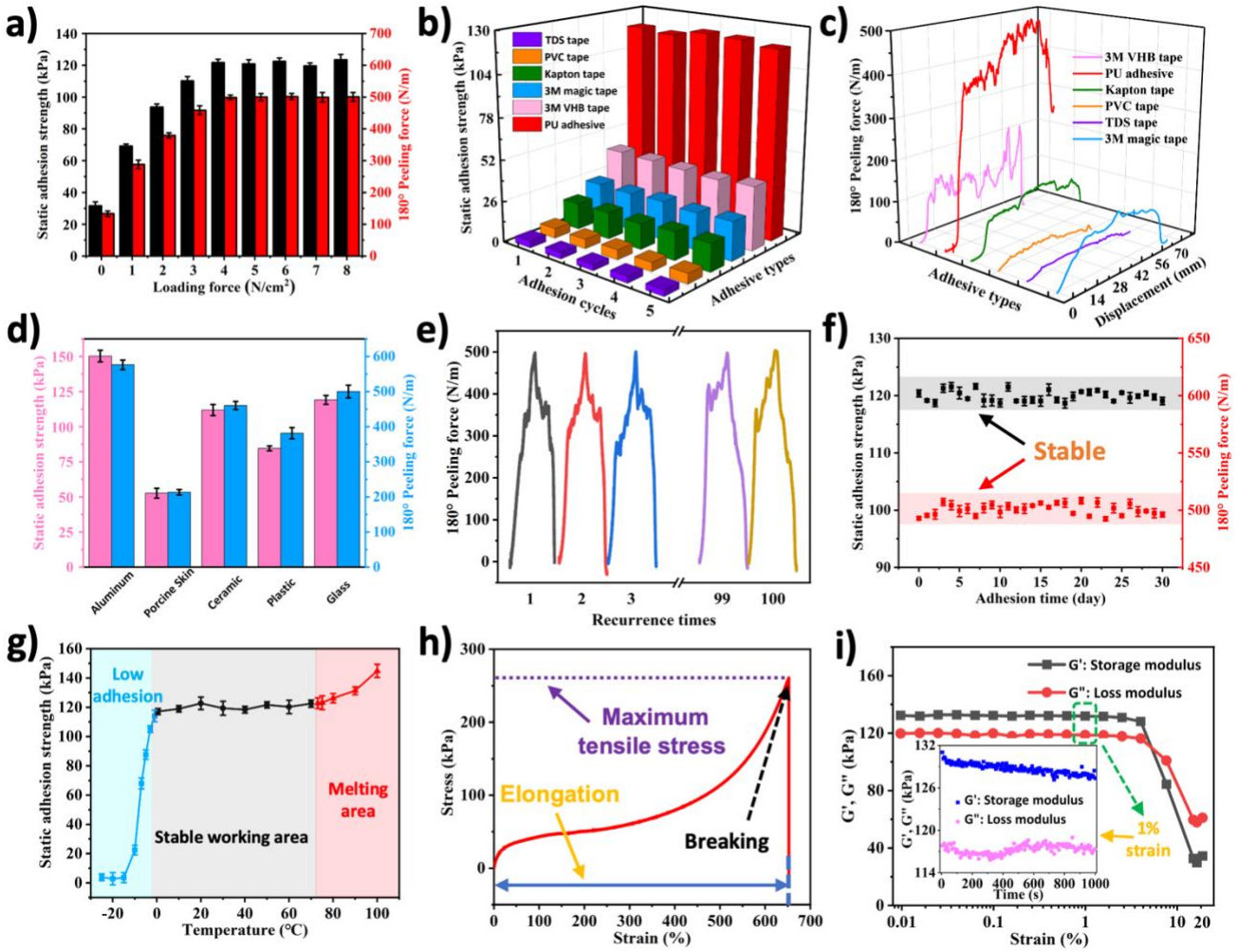


**Figure 2.** a) The relationship between the static adhesion performance/180° peeling force and joining force of the PU adhesive tape. b) Static adhesion strength on glass substrates for different adhesives, including PU adhesive, 3M magic tape, 3M VHB tape, PVC tape, Kapton tape, and traditional double-sided tape (TDS tape). c) 180° peeling force on glass substrates for different adhesives, including PU adhesive, 3M magic tape, 3M VHB tape, PVC tape, Kapton tape and traditional double-sided tape (TDS tape). d) Static adhesion strength and 180° peeling force of PU adhesive on various solid surfaces (aluminum, porcine skin, ceramic, plastic, and glass). e) Relationship between the number of bonding-debonding cycles and the 180° peeling force for PU adhesives. f) Relationship between the reusability (adhesion) and adhesion time of PU adhesive. g) Relationship between the static adhesion strength and working temperature of the adhesive tape. h) Typical tensile stress–strain curve for the PU adhesive. i) Variation of the storage modulus (G′) and loss modulus (G″) of PU adhesives with strain.

**Transparency &Wet-cleaning property**

Adhesives exhibiting strong adhesion and durable optical transparency are essential to bond electronic optical devices. We took photos of PU adhesives after different adhesion times and characterized their light transmittance at wavelengths ranging from 200 nm to 800 nm (Figure 3a and b). Even after 1

month, the transparency of the PU adhesives remained higher than 90% for wavelengths larger than 400 nm (high optical transparency). This indicates that the light transmittance of the adhesive is stable and does not change significantly with adhesion time. In addition, transparency increases with stretching (Figure 3c). This is due to the decrease in tape's thickness, which shortens the light absorption path, leading to a higher light transmittance.

Generally, when an adhesive tape adheres to a dusty solid surface, the dust will stay on the tape's surface, decreasing adhesion and transparency. In this regard, we define $L_A = \frac{\delta_0 - \delta_1}{\delta_0} * 100\%$ (Formula 1), and $L_T = \frac{\lambda_0 - \lambda_1}{\lambda_0} * 100\%$ (Formula 2) as the loss of adhesion and transparency after contamination with dust. Where $\delta_0$ and $\delta_1$ are the static adhesion, and $\lambda_0$ and $\lambda_1$ are the light transmittance before and after contamination, respectively. Our PU adhesive overcomes this limitation through its excellent wet-cleaning performance (Figure S16, Video S4). The wet-cleaning ability is quantified as: $R_A = \frac{\delta_2 - \delta_1}{\delta_0 - \delta_1} * 100\% = \frac{L_{A2}}{L_{A1}} * 100\%$ (Formula 3), $R_T = \frac{\lambda_2 - \lambda_1}{\lambda_0 - \lambda_1} * 100\% = \frac{L_{T2}}{L_{T1}} * 100\%$ (Formula 4). Where $R_A$ and $R_T$ refer to the recovery efficiency of static adhesion strength and light transmittance; $\delta_0, \delta_1$ and $\delta_2$ are the static adhesions and $\lambda_0, \lambda_1$ and $\lambda_2$ are the light transmittances of original, contaminated and wet-cleaned PU adhesives; $L_{A1}$ and $L_{A2}$ are the static adhesion and $L_{T1}$ and $L_{T2}$ are the light transmittance loss rate before and after wet-cleaning. Figure 3d shows the static adhesion and light transmission performance of 5 PU adhesives (different degrees of pollution) before and after wet-cleaning. After wet-cleaning and drying, their static adhesion and light transmittance performance were significantly improved, and the loss rates were less than 8%. The relative recovery efficiency of static adhesion and light transmittance for the five adhesives tested are above 90%. The unrecovered loss is mainly caused by the smaller dust particles, which can get embedded into the adhesive's micro/nano pores and couldn't be removed during wet-cleaning (Figure

S17). The moisture left on the adhesive tape after cleaning would cause a large decrease in the adhesive's static adhesion performance (Figure S18). Therefore, the wet-cleaned tape needs to be fully dried before testing its static adhesion and light transmittance.

In order to further clarify which dust characteristics affects the tape's wet-cleaning performance, we use hydrophilic ($Al_2O_3$) and hydrophobic particles (polystyrene: PS) with average particle sizes of 1, 5 and 8 μm to simulate particle pollution (Figure S19).[33] The particles were packaged in dry air and used as supplied, all tests were performed in a clean room. Since the adhesion of the wet-cleaned adhesive is affected by the drying conditions (Figure S18), we first studied the relationship between recovery efficiency, drying time and drying temperature. As shown in Figure 3e, 3f, for a constant drying temperature, the static adhesion strength recovers gradually to a maximum with increasing drying time, and then remains stable. Moreover, the higher the drying temperature, the shorter the drying time required to reach maximum recovery. This experiment revealed that the wet-cleaning performance is unrelated to the hydrophilicity/ hydrophobicity of the dust particles (diameter 8 μm). The wet-cleaning efficiencies for PU adhesive tapes contaminated by these two microparticles are both about 98% (Figure 3e, 3f). Then, we explored the effect of particle size on the wet-cleaning efficiency (Figure 3g, 3h). The drying temperature and drying time were kept as 50 ℃ and 3 h respectively. The larger the particle size of the contaminants, the more efficient was the wet-cleaning. This is because small particles (1 μm) are more likely to embed into the micro/nano pores on adhesive's surface. In all cases recovery of adhesion strength and light transmittance was above 90%. Although, it was affected by the particle size, it did not depend on the nature of the particles (Figure 3g, 3h). In addition, the recovery efficiencies remain stable during repeated contamination-cleaning cycles (Figure 3g, 3h).

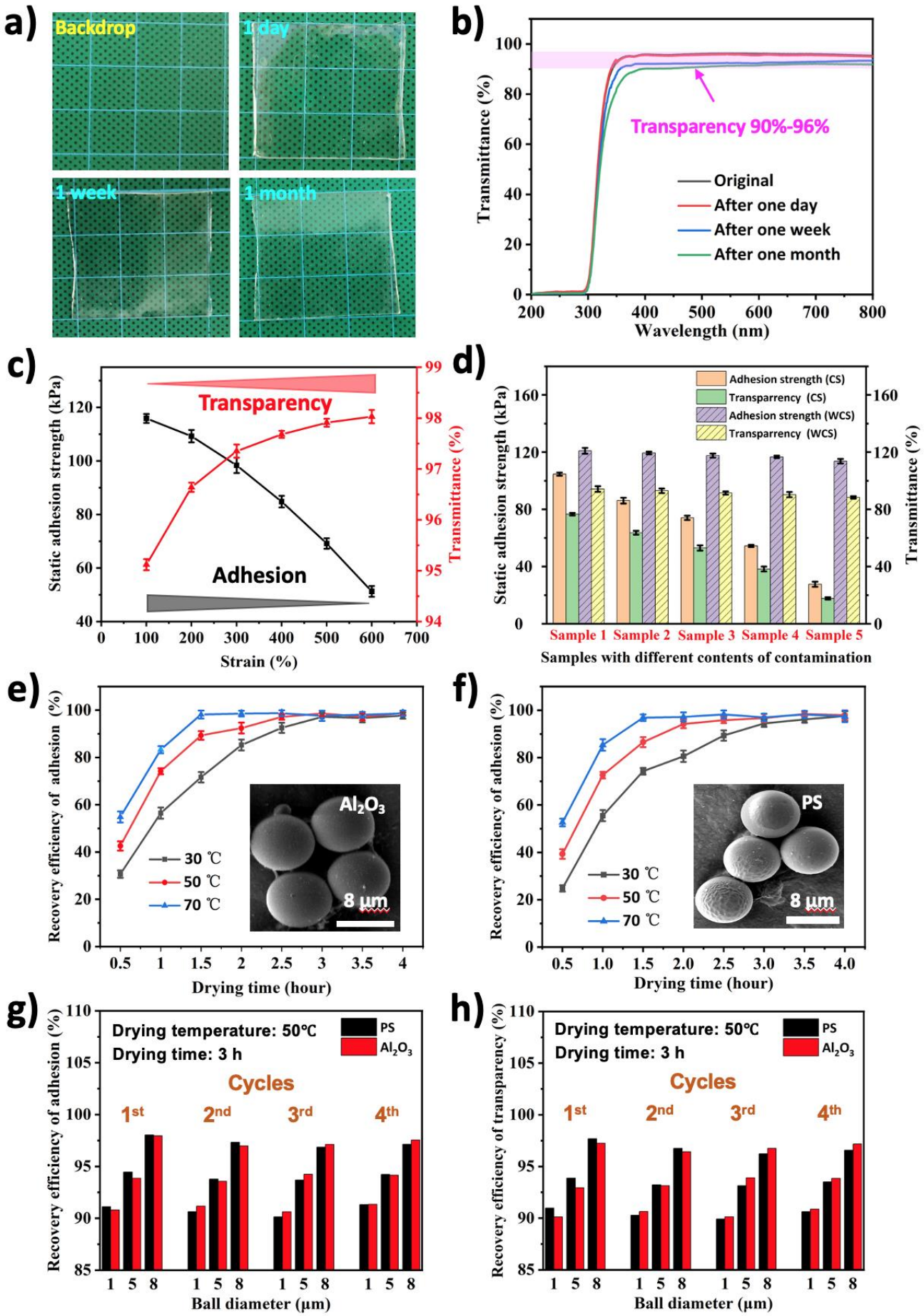
a)
Backdrop
1 day
1 week
1 month
b)
Transmittance (%)
Wavelength (nm)
Transparency 90%-96%
Original
After one day
After one week
After one month
c)
Static adhesion strength (kPa)
Transmittance (%)
Strain (%)
Transparency
Adhesion
d)
Static adhesion strength (kPa)
Transmittance (%)
Adhesion strength (CS)
Transparrency (CS)
Adhesion strength (WCS)
Transparrency (WCS)
Sample 1
Sample 2
Sample 3
Sample 4
Sample 5
Samples with different contents of contamination
e)
Recovery efficiency of adhesion (%)
Drying time (hour)
30 ℃
50 ℃
70 ℃
Al2O3
8 μm
f)
Recovery efficiency of adhesion (%)
Drying time (hour)
30 ℃
50 ℃
70 ℃
PS
8 μm
g)
Recovery efficiency of adhesion (%)
Drying temperature: 50℃
Drying time: 3 h
PS
Al2O3
Cycles
1st
2nd
3rd
4th
Ball diameter (μm)
h)
Recovery efficiency of transparency (%)
Drying temperature: 50℃
Drying time: 3 h
PS
Al2O3
Cycles
1st
2nd
3rd
4th
Ball diameter (μm)

**Figure 3.** a,b) Transparency stability of PU adhesives after long-term under ambient conditions. c) Relationship between the static adhesion performance/transparency and elongation of the adhesive tape. d) Adhesion performance and transparency of samples with different contamination levels before and after wet cleaning. e) Percentage of adhesion recovery with drying time at different drying temperatures after cleaning a contamination with hydrophilic 8 μm $Al_2O_3$ particles. f) Percentage of adhesion recovery with drying time at different drying temperatures after cleaning a contamination with hydrophobic 8μm PS spheres. g) Adhesion recovery depended on the diameter of the contaminant particles. h) Variation of the recovery in transparency as a function of the size of the contaminant particles.

## Discussion

The strong adhesion exhibited by the PU tape derives from two key features. One is the negative pressure generated by the micro/nano pores, and the other is the physical forces such as hydrogen bonding, metal coordination, hydrophobic interactions (Figure S20), and π-π stacking & cation-π interactions (Figure 1c, S6). The effect of the negative pressure is revealed by the static adhesion tests on silicon wafers, which shows stronger bonding with increasing joining pressure (Figure S21). Since the surface of the silicon wafer is smooth at the atomic scale, enhanced adhesion does not result from an increase in the contact area, which proves the existence of the negative pressure effect.

In practical applications, the solid surfaces to which the adhesive tape adheres are microscopically rough (Figure 4a). As a result, there are different contact states between PU adhesives and solid surfaces. If no external force is applied, the adhesive tape only contacts the peaks in the surface roughness (Figure 4b, state I). As the external force/pressure is increased slowly, the PU adhesive deforms and gradually fills the cavities in the rough surface, thereby increasing the contact area, which also increases the area of physical interaction (Figure 4b, state II). Meanwhile, as the pressure increases, the adhesive that was previously in contact with the surface would expel the gas in the micro/nano pores generating negative pressure (Figure 4b, state II). With the continuous increase of the external forces, the maximum contact area will be reached. Simultaneously, more gas in micro/nano pores is

forced out to increase the negative pressure (Figure 4b, state III). Finally, the gas in the remaining micro/nano pores would also be discharged and closely attach to solid surface with a further increase of the applied force/pressure, thereby forming a strong negative pressure (similar to octopus sucker) to improve adhesion strength (Figure 4b, state IV). Since the PU adhesive undergoes plastic deformation, the adhesive would not shrink after removing the joining force, retaining close contact with the substrate (Figure S5, S22).

When measuring the static adhesion strength, the contacting area between solid surface and adhesive tape would provide a viscous resistance opposite to dragging force to hinder the movement of the PU adhesive (Figure 4c). The viscous resistance is positively related to the contacting area and the negative pressure effect, so the PU tape exhibits pressure-sensitive property. The contribution of the negative pressure to the adhesion strength is much higher than the physical interactions (Fig. S21), this is why the static adhesion of the PU adhesive tape is stronger than commercial products that only rely on the later. If the adhesive is peeled from a solid surface, the viscous resistance of the adhesive is only provided by a small area near the separation interface, which is also pressure-sensitive (Figure 4c). During peeling off, air would re-enter the micro/nano pores without destroying them, therefore the tape is reusable and its performance does not diminish after several bonding-debonding cycles (Figure S23).

If the adhesive tape is contaminated by dust, the contacting area between the adhesive and the solid decreases (Figure 4e), and adhesion is significantly reduced. The tape can then be cleaned with water. The interactions between water molecules and PU adhesive would replace the intermolecular interactions between adhesive tape and dust, and the dust would be taken away by the flowing water (Figure S16, 17). However, a water film would cover the outermost layer and fill micro/nano pores of

the tape at the same time. If the PU tape is bonded to a solid surface at this stage, there will be a liquid film between the adhesive and the surface, leading to poor adhesion (Figure 4e). With drying, the moisture on the adhesive tape is eliminated. However, small dust particles will still remain in the tape's micro/nano pores (Figure S17), causing a slight loss of adhesion. These residual micro-particles also decrease the transparency of the adhesive (Figure 3d).

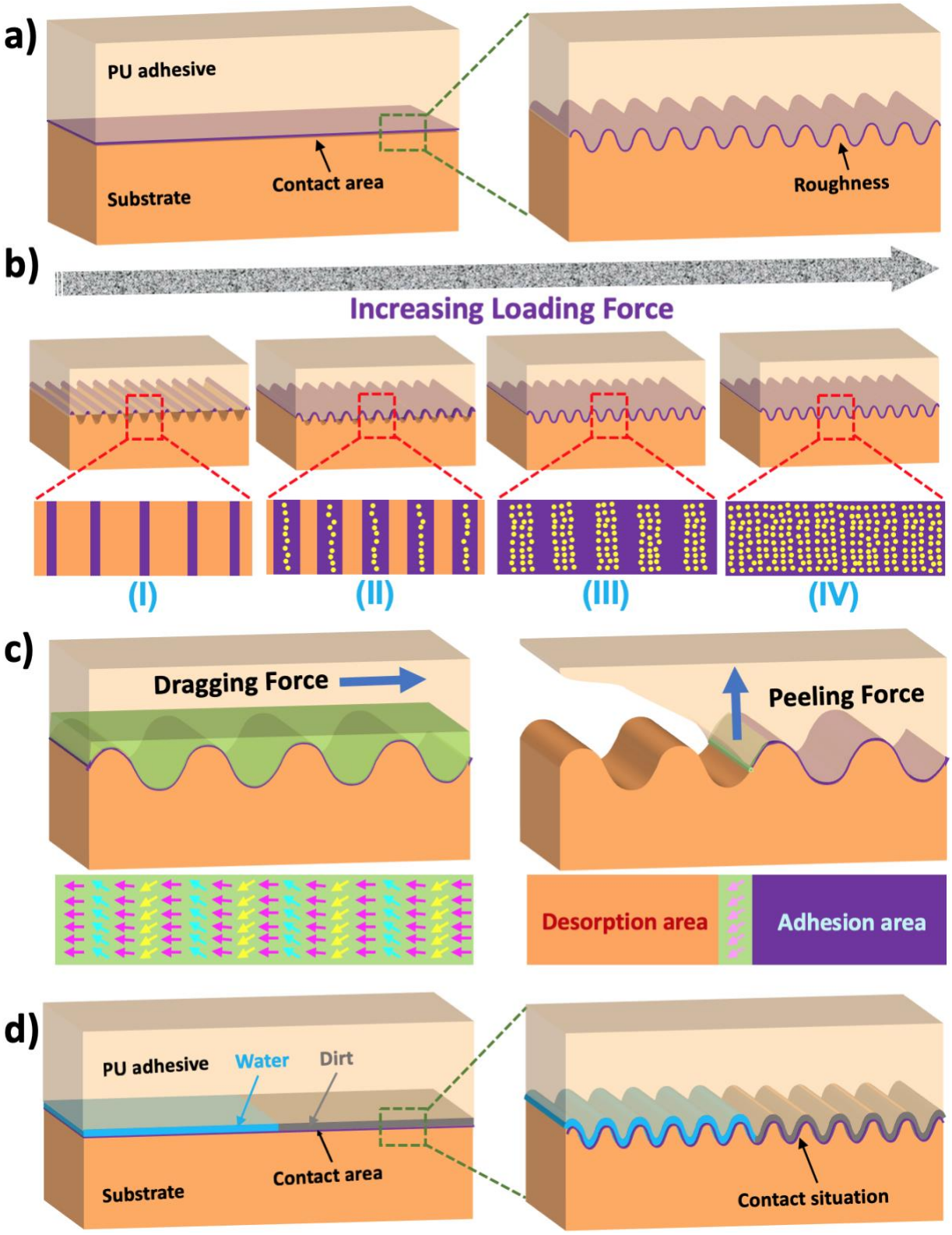


**Figure 4.** a) Schematic showing the difference between joining to a flat or rough solid surface. b) Schematic of showing the evolution of the contact area on a rough surface as a function of the joining force. c) Resistance force on the contacting area when testing static adhesion strength/180° peeling force. d) Contact between PU adhesive and solid surfaces when contaminated by dirt or liquid.

**Conclusion**

In summary, we have prepared a pressure-sensitive polyurethane tape that exhibits strong adhesion to organic and inorganic materials, (120 kPa) and high transparency (>90%). It also has superior dynamic adhesion to biological tissues. Moreover, it can be easily cleaned with water to eliminate contamination and restore adhesion. The outstanding cleaning capabilities (90-95% recovery) and long-lasting service life (more than 100 cycles) open opportunities for application in a wide range of fields. This work provides a new way for the design and preparation of bio-inspired dry adhesives.

## Experimental Section

### Materials

Polyether triol (molecular weight of 6000), Polyether glycol (molecular weight of 2000 and 4000) were purchased from KUKDO Chemical Co. Ltd. Organic Bismuth and Organic Zinc were purchased from Shanghai Shepherd Chemical Company. PPE defoamer was purchased from Suzhou Beston Chemical Co., Ltd. Diphenylmethane diisocyanate was purchased from Nantong Runzhou Chemical Co., Ltd. UV-320, diethyl phosphite, were purchased from Shanghai Aladdin Biochemical Technology Co. Ltd. All reagents were used directly and did not require further purification. Cells and other materials for determining the biocompatibility of the adhesive tape were provided by Jinhao Gao group, Xiamen University.

### Synthesis of polyurethane adhesive tape

In this experiment, polyether triol (molecular weight of 6000, 500 g), polyether glycol (molecular weight of 2000, 250 g) and polyether glycol (molecular weight of 4000, 250 g) were mixed first. Next, organic bismuth (2 g), organic zinc (2 g), UV-320 resistant UV additives (10 g), diethyl phosphite antioxidant (10 g) and PPE defoamer (5 g) are added and continue to mix to obtain the first reaction component. Then, the first reaction component was put into the first airtight container of the glue mixing instrument and vacuum for 20 minutes. After that, 200g diphenylmethane diisocyanate solution with a mass fraction of 7% was added into the second closed container of the glue mixing instrument, and mix the first reaction component and the second reaction component in the glue mixing device. Finally, the mixture mixed by the glue mixing instrument is applied to the polyurethane substrate, followed by reacting and curing at 70 °C for 8 minutes to obtain a polyurethane adhesive.

### Biocompatibility evaluation of PU adhesive

The biocompatibility of the adhesive tape was evaluated according to the standards of a cytotoxicity test in vitro recommended in GB/T 16886.

### Characterization

Scanning electron microscope (SEM) images were taken with a JEOL JSM-6700F scanning electron microscope. Photographs and videos were taken with a SLR camera (Canon-EOS-760D). Images of the micro/nano pores in the PU adhesive were taken using an optical microscope (Zeiss GeminiSEM

500). Contact angles of the electrolyte were taken with the Contact Angle System OCA 20 (Dataphysics, Germany). Tensile and compression experiments are performed under a universal tester (INSTRON 5567). Fourier- transform infrared spectroscopy (FTIR) was performed on a Bruker Tensor 27 spectrophotometer. Chemical analysis by Energy Dispersive Spectroscopy (EDS) was performed in a field emission scanning electron microscope (Oxford instruments INCA x-act). Static adhesion and peeling adhesion were tested using a texture analyzer (CT3-1000). Cell images were taken with an inverted fluorescence microscope (AXIO OBSEVER A1). Dynamic rheological tests of PU adhesives were characterized at 25 ℃ using a DHR-2 Rotational Rheometer (TA, America) equipped with 25 mm parallel plates. The storage modulus (G′) and loss tangent (ratio of loss modulus G″ to storage modulus G′) of the adhesives were determined as the frequency ranging from 0.01 to 20 Hz at 1.0% strain amplitude.

**Supporting Information**

Supporting Information is available from the author.

**Acknowledgements**

This work was supported by the EPSRC Program Manufacture Using Advanced Powder Processes (MAPP)EP/P006566, the National Key R&D Program of China (2018YFA0209500) and the National Natural Science Foundation of China (21673197). Ming Li acknowledges financial assistance from Imperial College London, and granting him the “President Scholarship” (2019-2023). Qingwen Guan appreciates the support from the China Scholarship Council (2020-2023). We are grateful to Yifan Fan (Xiamen university) for his selfless dedication, discussion and assistance in this work.

**Author contributions**

Ming Li and Weijun Li conceived and designed the project, they contribute equally to this work. Qingwen Guan participated in the performance of the experiments. Dr. Jing Lv provided important suggestions for the cytotoxicity tests and guided this part of the work. Prof. Eduardo Saiz revised the content of article and provide some useful suggestions. All authors discussed the results and commented on the manuscript.

## References

1. Autumn, K.; Liang, Y. A.; Hsieh, S. T.; Zesch, W.; Chan, W. P.; Kenny, T. W.; Fearing, R.; Full, R. J., Adhesive force of a single gecko foot-hair. *Nature* **2000,** *405* (6787), 681-685.
2. Lee, H.; Um, D. S.; Lee, Y.; Lim, S.; Kim, H. j.; Ko, H., Octopus-inspired smart adhesive pads for transfer printing of semiconducting nanomembranes. *Adv. Mater.* **2016,** *28* (34), 7457-7465.
3. Baik, S.; Park, Y.; Lee, T.-J.; Bhang, S. H.; Pang, C., A wet-tolerant adhesive patch inspired by protuberances in suction cups of octopi. *Nature* **2017,** *546* (7658), 396-400.
4. Arzt, E.; Gorb, S.; Spolenak, R., From micro to nano contacts in biological attachment devices. *P. Natl. Acad. Sci.* **2003,** *100* (19), 10603-10606.
5. Eisner, T.; Aneshansley, D. J., Defense by foot adhesion in a beetle (Hemisphaerota cyanea). *P. Natl. Acad. Sci.* **2000,** *97* (12), 6568-6573.
6. Hansen, W. R.; Autumn, K., Evidence for self-cleaning in gecko setae. *P. Natl. Acad. Sci.* **2005,** *102* (2), 385-389.

7. Neubauer, J. W.; Xue, L.; Erath, J.; Drotlef, D.-M.; Campo, A. n. d.; Fery, A., Monitoring the contact stress distribution of gecko-inspired adhesives using mechano-sensitive surface coatings. *ACS Appl. Mater. Inter.* **2016,** *8* (28), 17870-17877.
8. Zhang, C.; Mcadams, D. A.; Grunlan, J. C., Nano/Micro-Manufacturing of Bioinspired Materials: a Review of Methods to Mimic Natural Structures. *Adv. Mater.* **2016,** *28* (30), 6292-6321.
9. Autumn, K.; Sitti, M.; Liang, Y. A.; Peattie, A. M.; Hansen, W. R.; Sponberg, S.; Kenny, T. W.; Fearing, R.; Israelachvili, J. N.; Full, R. J., Evidence for van der Waals adhesion in gecko setae. *P. Natl. Acad. Sci.* **2002,** *99* (19), 12252-12256.
10. Raut, H. K.; Baji, A.; Hariri, H. H.; Parveen, H.; Soh, G. S.; Low, H. Y.; Wood, K. L., Gecko-inspired dry adhesive based on micro–nanoscale hierarchical arrays for application in climbing devices. *ACS Appl. Mater. Inter.* **2018,** *10* (1), 1288-1296.
11. Wang, S.; Fang, Y.; He, H.; Zhang, L.; Li, C. a.; Ouyang, J., Wearable Stretchable Dry and Self-Adhesive Strain Sensors with Conformal Contact to Skin for High-Quality Motion Monitoring. *Adv. Funct. Mater.* **2020**, 2007495.
12. Kim, J.; Kim, D. W.; Baik, S.; Hwang, G. W.; Kim, T. i.; Pang, C., Snail-Inspired Dry Adhesive with Embedded Microstructures for Enhancement of Energy Dissipation. *Advanced Materials Technologies* **2019,** *4* (11), 1900316.
13. Chun, S.; Kim, D. W.; Baik, S.; Lee, H. J.; Lee, J. H.; Bhang, S. H.; Pang, C., Conductive and Stretchable Adhesive Electronics with Miniaturized Octopus-Like Suckers against Dry/Wet Skin for Biosignal Monitoring. *Adv. Funct. Mater.* **2018,** *28* (52), 1805224.
14. Kim, D. W.; Baik, S.; Min, H.; Chun, S.; Lee, H. J.; Kim, K. H.; Lee, J. Y.; Pang, C., Highly permeable skin patch with conductive hierarchical architectures inspired by amphibians and octopi for omnidirectionally enhanced wet adhesion. *Adv. Funct. Mater.* **2019,** *29* (13), 1807614.
15. Gu, G.; Zou, J.; Zhao, R.; Zhao, X.; Zhu, X., Soft wall-climbing robots. *Science Robotics* **2018,** *3* (25).
16. Hensel, R.; Moh, K.; Arzt, E., Engineering micropatterned dry adhesives: from contact theory to handling applications. *Adv. Funct. Mater.* **2018,** *28* (28), 1800865.
17. He, Q.; Yang, X.; Wang, Z.; Zhao, J.; Yu, M.; Hu, Z.; Dai, Z., Advanced electro-active dry adhesive actuated by an artificial muscle constructed from an ionic polymer metal composite reinforced with nitrogen-doped carbon nanocages. *J. Bionic Eng.* **2017,** *14* (3), 567-578.
18. Hu, H.; Tian, H.; Shao, J.; Li, X.; Wang, Y.; Wang, Y.; Tian, Y.; Lu, B., Discretely supported dry adhesive film inspired by biological bending behavior for enhanced performance on a rough surface. *ACS Appl. Mater. Inter.* **2017,** *9* (8), 7752-7760.
19. Hu, S.; Xia, Z., Rational design and nanofabrication of gecko-inspired fibrillar adhesives. *Small* **2012,** *8* (16), 2464-2468.
20. Raut, H. K.; Dinachali, S. S.; Loke, Y. C.; Ganesan, R.; Ansah-Antwi, K. K.; Gora, A.; Khoo, E. H.; Ganesh, V. A.; Saifullah, M. S.; Ramakrishna, S., Multiscale ommatidial arrays with broadband and omnidirectional antireflection and antifogging properties by sacrificial layer mediated nanoimprinting. *ACS Nano* **2015,** *9* (2), 1305-1314.
21. Kustandi, T. S.; Samper, V. D.; Yi, D. K.; Ng, W. S.; Neuzil, P.; Sun, W., Self-assembled nanoparticles based fabrication of gecko foot-hair-inspired polymer nanofibers. *Adv. Funct. Mater.* **2007,** *17* (13), 2211-2218.
22. Ranzani, T.; Russo, S.; Bartlett, N. W.; Wehner, M.; Wood, R. J., Increasing the dimensionality of soft microstructures through injection-induced self-folding. *Adv. Mater.* **2018,** *30* (38), 1802739.

23. Qu, L.; Dai, L.; Stone, M.; Xia, Z.; Wang, Z. L., Carbon nanotube arrays with strong shear binding-on and easy normal lifting-off. *Science* **2008,** *322* (5899), 238-242.
24. Röhrig, M.; Thiel, M.; Worgull, M.; Hölscher, H., Hierarchical Structures: 3D Direct Laser Writing of Nano-and Microstructured Hierarchical Gecko-Mimicking Surfaces (Small 19/2012). *Small* **2012,** *8* (19), 2918-2918.
25. Paretkar, D.; Kamperman, M.; Martina, D.; Zhao, J.; Creton, C.; Lindner, A.; Jagota, A.; McMeeking, R.; Arzt, E., Preload-responsive adhesion: effects of aspect ratio, tip shape and alignment. *Journal of the Royal Society Interface* **2013,** *10* (83), 20130171.
26. Heinzmann, C.; Weder, C.; de Espinosa, L. M., Supramolecular polymer adhesives: advanced materials inspired by nature. *Chem. Soc. Rev.* **2016,** *45* (2), 342-358.
27. Rizzo, N.; Gardner, K.; Walls, D. e. a.; Keiper-Hrynko, N.; Ganzke, T.; Hallahan, D., Characterization of the structure and composition of gecko adhesive setae. *Journal of The Royal Society Interface* **2006,** *3* (8), 441-451.
28. Bauer, C. T.; Kroner, E.; Fleck, N. A.; Arzt, E., Hierarchical macroscopic fibrillar adhesives: in situ study of buckling and adhesion mechanisms on wavy substrates. *Bioinspiration & biomimetics* **2015,** *10* (6), 066002.
29. Li, W.; Li, Y.; Sheng, M.; Cui, S.; Wang, Z.; Zhang, X.; Yang, C.; Yu, Z.; Zhang, Y.; Tian, S., Enhanced adhesion of carbon nanotubes by dopamine modification. *Langmuir* **2019,** *35* (13), 4527-4533.
30. Liu, X.; Zhang, Q.; Gao, Z.; Hou, R.; Gao, G., Bioinspired adhesive hydrogel driven by adenine and thymine. *ACS Appl. Mater. Inter.* **2017,** *9* (20), 17645-17652.
31. Liu, X.; Zhang, Q.; Gao, G., Bioinspired adhesive hydrogels tackified by nucleobases. *Adv. Funct. Mater.* **2017,** *27* (44), 1703132.
32. Li, X.; Tao, D.; Lu, H.; Bai, P.; Liu, Z.; Ma, L.; Meng, Y.; Tian, Y., Recent developments in gecko-inspired dry adhesive surfaces from fabrication to application. *Surface Topography: Metrology and Properties* **2019,** *7* (2), 023001.
33. Li, M.; Xu, Q.; Wu, X.; Li, W.; Lan, W.; Heng, L.; Street, J.; Xia, Z., Tough reversible adhesion properties of a dry self-cleaning biomimetic surface. *ACS Appl. Mater. Inter.* **2018,** *10* (31), 26787-26794.

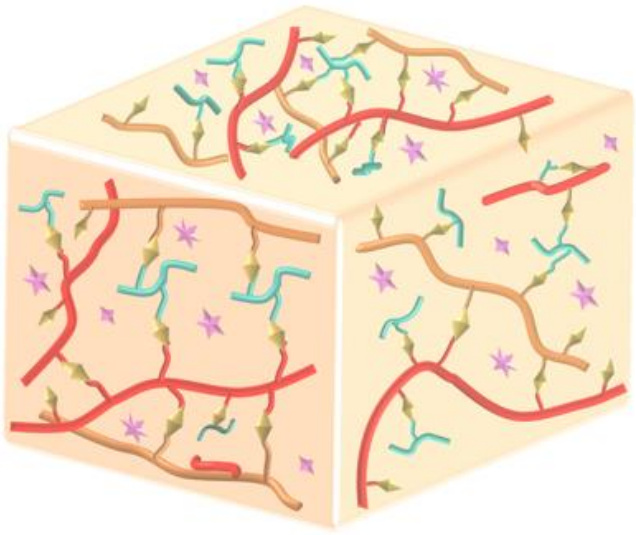

**Table of Contents**